

# Completing the Viability Demonstration of Direct-Drive IFE Target Engagement and Assessing Scalability to a Full-Scale Power Plant

Lane C. Carlson, Mark S. Tillack, Jeremy Stromsoe, Neil B. Alexander, G. W. Flint, Daniel T. Goodin, and Ronald W. Petzoldt

**Abstract**—A significant challenge for the successful implosion of direct-drive inertial fusion energy targets is the repeated alignment of multiple laser beams on moving targets with accuracy on the order of  $20\ \mu\text{m}$ . Adding to the difficulty, targets will be traveling up to  $100\ \text{m/s}$  through a chamber environment that may disturb their trajectories. In the High Average Power Laser program, we have developed a target tracking and engagement system that is capable of meeting the goals for an inertial fusion power plant. The system consists of separate axial and transverse target detection techniques and a final correction technique using a short-pulse laser to interrogate the target's position 1–2 ms before a chamber center. Steering mirrors are then directed to engage the target at the chamber center. Over the past few years, we have constructed and improved upon an integrated tabletop demonstration operating at reduced speeds and path lengths. In August 2007, initial engagement of moving targets in air using a simulated driver beam was  $150\text{-}\mu\text{m}$  rms. Since then, we have taken an encompassing look at all error sources that contribute to the overall engagement error. By focusing on those individual component errors that have the most influence and improving their accuracy, we have substantially reduced the overall engagement error. In August 2008, we had achieved an engagement of  $42\text{-}\mu\text{m}$  rms in air by using this approach, and in March 2009,  $34\text{-}\mu\text{m}$  rms in vacuum. The final elements, which we believe are necessary to meet our goal, necessitate engaging lightweight targets in a prototypic vacuum environment with an understanding of the scalability of demonstration-scale errors to full-scale errors. In this paper, we present the latest improvements from the identification and reduction of errors and the resulting engagement data demonstrating near completion of the viability demonstration of direct-drive target engagement to  $20\ \mu\text{m}$ .

**Index Terms**—Component, glint system, Poisson spot, target tracking and engagement.

## I. INTRODUCTION

THE HIGH Average Power Laser direct-drive inertial fusion energy (IFE) power plant consists of an array of 60 driver beams to deliver an intense energy pulse directly onto the target. Targets must be injected into the chamber with a placement accuracy of  $\pm 1\ \text{mm}$  at a standoff distance of  $\sim 20\ \text{m}$ .

Manuscript received June 25, 2009; revised October 8, 2009. First published January 12, 2010; current version published March 10, 2010.

L. C. Carlson, M. S. Tillack, and J. Stromsoe are with the Center for Energy Research, University of California, San Diego, La Jolla, CA 92093 USA (e-mail: lcarlson@ucsd.edu; mtillack@ucsd.edu; jstromsoe@gmail.com).

N. B. Alexander, G. W. Flint, D. T. Goodin, and R. W. Petzoldt are with General Atomics, San Diego, CA 92121 USA (e-mail: neil.alexander@gat.com; gflint@swcp.com; dan.goodin@gat.com; ronald.petzoldt@gat.com).

Digital Object Identifier 10.1109/TPS.2009.2037423

The required engagement accuracy of all driver beams on the target is  $\pm 20\ \mu\text{m}$  [1].

We have developed a target tracking and engagement concept to meet these requirements and have assembled a tabletop experiment that engages an injected target on the fly using a steerable simulated driver beam [2]. The system continuously tracks the target along its trajectory and makes a final steering correction that is made relative to the target itself. The tabletop experiment has demonstrated proof of principle at reduced speeds and distances and will establish the concepts' feasibility for a full-scale power plant.

Since the initial engagement accuracy of  $150\ \mu\text{m}$ , we have reduced the individual component errors and improved the glint return (GR) imaging system, which has resulted in improved engagement to less than  $50\ \mu\text{m}$ . With all improvements already in place and those presented in this paper, we expect to meet our  $20\text{-}\mu\text{m}$  accuracy goal and complete the viability demonstration of IFE target engagement. We also present a look into the scalability of the engagement precision achieved on the demonstration to a full-size power plant.

## II. SYSTEM DESIGN AND OVERVIEW

The target tracking and engagement design is composed of three main subsystems, as shown in Fig. 1 and described in more detail in [2]. First, a laser-based continuous tracking system sights along the target's flight path and uses position information from the target's Poisson spot to determine the target's transverse position. Second, a system using discrete crossing sensors provides the necessary timing to trigger a glint laser, driver beam laser, coincidence camera, and a verification camera. Finally, a short-pulse glint laser illuminates the target a few milliseconds before it reaches the chamber center, thus using the GR from the target itself as the final reference point for aligning the driver beams immediately before engagement. In the presteering scenario described in [3], information from the Poisson spot presteers the mirror to take up any gross position errors, while the glint system makes the final small steering correction.

## III. IDENTIFICATION AND REDUCTION OF ERRORS

At the end of 2008, the best engagement achieved was  $42\text{-}\mu\text{m}$  rms in air with heavy targets [3]. At that time, the demonstration was on the cusp of moving into a vacuum chamber, which is a

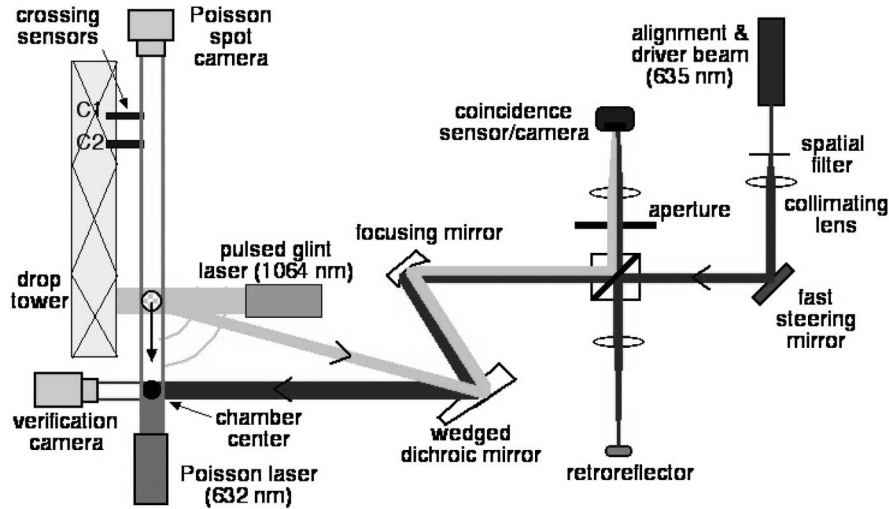


Fig. 1. Schematic of integrated target tracking and engagement demonstration. Focusing mirror to the chamber center is 2 m; drop tower is ~2 m tall (figure not to scale).

TABLE I  
ERROR CONTRIBUTION LIST

Subsystem	Oct. 2008 Errors ( $1\sigma$ )			April 2009 ( $1\sigma$ )		
	X ( $\mu\text{m}$ )	Y ( $\mu\text{m}$ )	Z ( $\mu\text{m}$ )	X ( $\mu\text{m}$ )	Y ( $\mu\text{m}$ )	Z ( $\mu\text{m}$ )
Poisson spot centroiding	(18)	(15)	6	(2)	(3)	1
Glint return	2	-	3	4	-	4
Verification algorithm	5	-	4	(4)	-	(4)
Mirror pointing	12	-	12	3	-	5
Timing prediction	-	-	35	-	-	(20)
Transverse target motion	24	(24)	10	5	(7)	5
Target diameter variation	3	(3)	3	4	(4)	4
Dynamic steering mirror	-	-	-	5	-	5
Calibration drift/error	-	-	-	12	-	12
Target eng. error (rms, compiled)	27	-	38	15	-	16
Target eng. error (rms, observed)	30	-	29	24	-	24
Total eng. error (total rms, observed)	42 $\mu\text{m}$			34 $\mu\text{m}$		

All errors converted to target space, errors in () do not contribute to the compiled error, Z-axis is axial to the target's trajectory, X and Y axis are transverse.

more prototypic environment of an actual power plant chamber than ambient air.

As the experiment progressed, we assembled a list of errors associated with every component of the tracking and engagement system that is believed to be a contributor to the overall engagement error (Table I), as first compiled in [3]. By individually testing and improving the errors on the component level, we aspired to improve the overall integrated target engagement error, as shown in Fig. 2.

The methods used to characterize the errors of the individual subsystems mainly utilized a stationary target to fix the target motion variable and isolate the subsystem being tested. Isolating a single subsystem eliminates some variables and incorporates individual components that are tied together to create a subsystem. For example, the Poisson spot subsystem incorporates a helium–neon laser that may wander and drift, optics and mirrors that may drift due to thermal fluctuations, a beam that propagates through air and vacuum that may waver due to index of refraction gradients, and a computer looking at this beam on a camera and computing the centroid. The testing

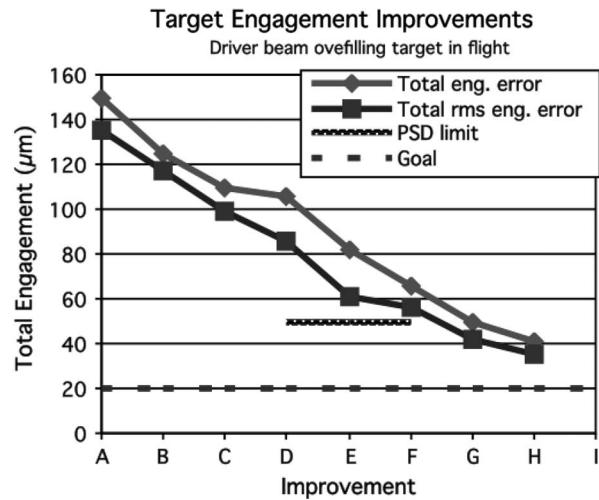


Fig. 2. Stepwise improvement graph with effect on the overall target engagement results. (A) Initial setup, 4:1 magnification, and defocused GR. (B) Focused GR. (C) Focused GR and small aperture. (D) 1:1 magnification. (E) 1:1 magnification, improved steering calibration. (F) Glint camera that replaces position-sensitive diode (PSD). (G) Stable beam splitter and small delta steering. (H) Vacuum chamber. (I) (Anticipated) Thermal drift and electrical noise eliminated.

method for this subsystem involves the laser beam overfilling a stationary target and taking a standard deviation of the centroid of the spot over numerous readings. The error of this subsystem, including all its individual components that make up the subsystem, is reported to be in the 2–3- $\mu\text{m}$  range. Each subsystem is similarly tested on a “bare-bones” subsystem-by-subsystem basis to ensure that all are contributing minimally to the overall engagement error.

The direction that stemmed from this most recent analysis focused on improving the Poisson spot wander, reducing electrical noise, specifically for the steering mirror, and moving the experiment to a vacuum environment. The sections that follow will focus on these areas of improvement as well as other new and inconspicuous error sources.

One new error source, which was brought into consideration with the installation of the vacuum chambers, is orthogonality.

There are multiple coordinate axes of various components in different coordinate spaces that all must be orthogonal to one another. The optical table on which the experiment lies, engagement verification camera, coincidence camera, Poisson spot camera, target calibration stage at the chamber center, steering mirror, and target dropping orientation must all be orthogonal to one another. One additional optic, a dove prism, was installed in the beam line midway between the wedge and the focusing mirror to accommodate adjustments. In addition, tests were conducted to ensure that the steering axes and the aforementioned cameras and sensors are all imaging orthogonal movement. For example, during calibration, an  $x$ -only movement of the target on the stage should solely correspond to an  $x$  movement on the coincidence camera with zero  $y$  component. Similarly,  $x$  steering of the mirror should only result in the  $x$  component of the beam moving on the verification camera. For the demonstration, orthogonality is convenient but most likely not possible in a multibeam power plant. Rotation of coordinate axes will need to be incorporated for the different beam lines coming into the chamber at various angles.

Two more issues that are currently under consideration and investigation are thermal drift and laboratory-wide electrical noise fluctuations. Thermal drift is prevalent throughout the day and moves the driver beam at the chamber center up to  $50\ \mu\text{m}$  in an open-loop steering configuration. This is correctable in a closed-loop alignment mode as the mirror locks on to a specific pixel on the coincidence camera and maintains its pointing to that location. During operation, the outgoing driver beam and incoming GR signal are common path and drift together. As it is, the thermal drift time scale is much longer than that of an engagement drop. However, any thermal fluctuations that change the GR location to steering voltage *calibration* are detrimental to target engagement. Further investigation is being conducted in this area, which has been identified in the past, but not actively pursued.

Ensuring that all electrical equipment, power supplies, and sensors for the experiment are on a common ground is crucial to minimizing electrical noise and ground loops. The ambient electrical noise in the laboratory can be monitored so that target engagement experiments are timed to coincide with minimal laboratory noise.

#### A. Transverse Tracking System

The Poisson spot tracking system provides the presteering system, movable area of interest, and wedge effect correction with a dependable and stable target position measurements at  $\sim 4$ -ms intervals [3]. The illuminating laser beam path propagation through air was reduced from  $\sim 7$  to  $\sim 2$  m. This involved assembling the laser and spatial filter on the tower itself (Fig. 3) and moving the tracking camera as close to the bottom chamber as possible. The resulting error of the Poisson spot of a stationary target on the camera was substantially reduced from 15- to  $3\text{-}\mu\text{m}$  stdev. For long path lengths, this error is dependent on the pointing stability of the laser light source and the propagation path in air. Provided that the Poisson spot beam propagates through a vacuum environment, this error is expected to scale consistently with the pointing stability of the

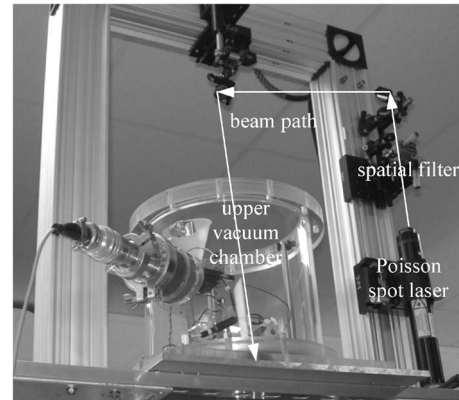


Fig. 3. Upper vacuum chamber on top of a support tower showing Poisson spot illumination beam being assembled and directed downward.

laser illumination source. For a power plant, this could be on the order of  $0.3\ \text{mm}$  for a beam propagating  $17\ \text{m}$ . The beam might require realignment to the center of the tracking camera.

#### B. Target Injection

For the time being, the demonstration uses gravity as its accelerator for injector means. The new tridropper mechanism as introduced in [3] allows for the dropping of multiple targets in vacuum. The recoil-free design transfers minimal transverse motion to the falling target by simultaneously activating three solenoids that pull away ruby-tipped pins riding on ball-bearing linear slides. The placement accuracy of stainless steel and brass BBs at the chamber center in vacuum is  $0.1\text{-mm}$  stdev, and for lightweight (approximately few milligrams) targets, it is  $0.4\text{-mm}$  stdev. The precise placement accuracy is helpful in reducing the final steering requirement for the mirror. For any full-scale power plant injector, whether pneumatic, mechanical, electrostatic, or gravity driven, a placement accuracy of  $\pm 1\ \text{mm}$  at the chamber center will permit an adequate field of view for target engagement.

The vacuum chamber is now operational, as shown in Fig. 4. It is constructed of clear  $1/2$ -in-thick acrylic and consists of two  $12$ -in diameter chambers with an extruded aluminum tube connecting the two. The crossing sensors are placed entirely in the vacuum and reside in the two black boxes on either side of the four-way cross. The top chamber houses the supply of targets and the dropping mechanism, while the lower chamber contains the calibration stage, catches the dropped targets, and allows the glint, Poisson, and driver laser beams to sight through its windows. Initial vacuum reached  $\sim 100$  mtorr with the lab's house vacuum system. Since then, a small turbomolecular pump has been installed to achieve  $< 0.5$  mtorr, a vacuum that might be expected for a power plant chamber operating at  $5\ \text{Hz}$ .

Transitioning to vacuum from air was needed to keep consistent with a prototypic power plant chamber. Vacuum permits the dropping of lightweight targets, which is nearly impossible in air due to drastic wake effects that buffet them as they fall. This curving effect, which influences the target between the glint location and the driver location ( $\sim 6\ \text{cm}$ ), has been reduced from  $24$ - to  $6\text{-}\mu\text{m}$  stdev, due to the better placement accuracy achieved in vacuum.

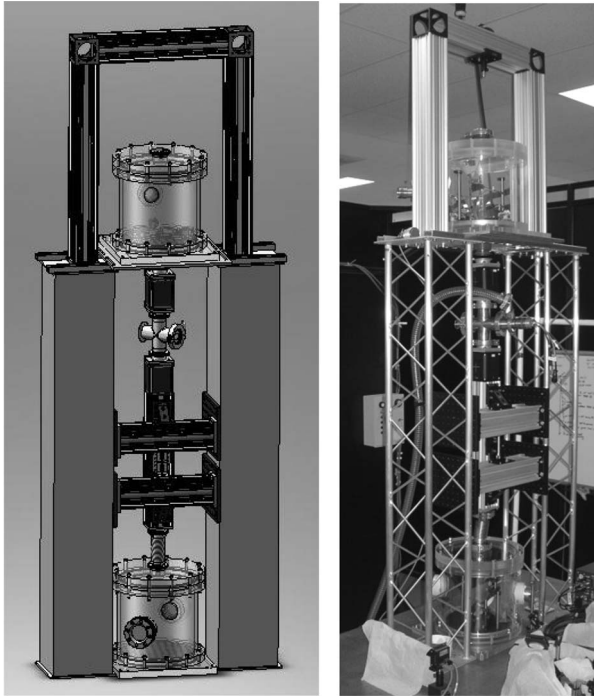


Fig. 4. Drop tower ( $\sim 2$  m tall) with upper and lower vacuum chambers. (Left) CAD drawing and (right) full assembly in the lab.

In anticipation of dropping lightweight targets in vacuum, we have begun measuring the diameter of various gold-coated poly alpha-methyl styrene (PAMS) targets using an optical technique with  $1\text{-}\mu\text{m}$  resolution. Most target engagement tests thus far have utilized heavy stainless steel or brass BBs of similar diameter and reflectivity as the PAMS targets. A more prototypic test will be the engagement of lightweight targets ( $2\text{--}10$  mg versus  $300$  mg). A necessary requirement, though, is a diameter variance of less than  $10\ \mu\text{m}$ . There will be a GR offset on the coincidence camera depending on the angle between the glint illumination laser and the GR signal. Since only one glint illumination source is needed for all the beam lines (the glint reflects off the target in  $4\pi$  sr), the offset will be known for every beam line depending on its geometric location as it enters the chamber. A chamber geometry where the glint illumination laser points directly into a driver beam line, i.e., the viewing angle is collinear with the illumination laser, will be avoided. A method of measuring the target's diameter on the fly and adjusting the mirror pointing accordingly to the known offset has been proposed, but not yet implemented.

### C. Glint System

The target moves several centimeters between the time the glint illuminates the target and the time the driver beam fires. The wedged dichroic mirror reflects the driver beam off the front surface and the GR signal off the back surface so that both beams relay back to the coincidence sensor [2]. The prior configuration held the aluminum mirror and long-pass filter separately on their individual mounts. The optics have since been epoxied together to create a more monolithic structure and to set the wedge angle permanently (Fig. 5). In this new

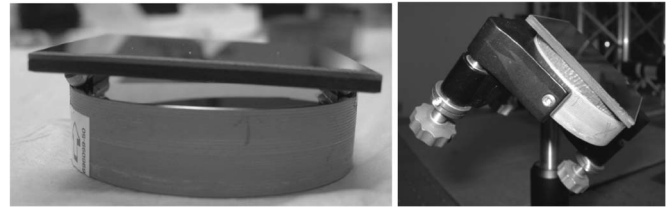


Fig. 5. Simulated monolithic wedged dichroic mirror (5-cm diameter).

configuration, the simulated optics more accurately represent a true monolithic wedged dichroic mirror, which is expected to be used in the final design. In terms of scalability, the precision of the target's glint position in the sensor space is simply a function of the intervening optical magnification (assuming insignificant gas density variations and no high-frequency vibrations of the optics), which can be preserved in a full-scale system.

### D. Beam Steering

The fast steering mirror's steering accuracy and stability have been improved. The mirror has been "desensitized" by voltage dividing the signal to the mirror controller. This allows the use of the entire dynamic range of the mirror controller ( $\pm 10$  V), in which the signal-to-noise ratio is much higher than when just a small portion ( $\pm 1$  V) is used. Electrical noise to the mirror has also been reduced by ensuring that a common ground exists between the steering signals and that no antennas or loops are created in the wiring harness. The combination of the desensitization and cleaning up the electrical noise has reduced the jitter of the driver beam at the chamber center from  $15\text{-}$  to  $4\text{-}\mu\text{m}$  stdev. The effect of the electrical noise on the beam's position is proportional to the maximum distance through which the beam must be steered, which is about  $\pm 1$  mm in the demonstration, as well as in a power plant.

The steering algorithm now more precisely computes the final steering voltage from the GR by taking the last steering voltage required to drive the alignment beam to the chamber center and then computing a delta steering voltage from that position to the GR. This is a more precise way to compute the final steering requirement, rather than using the calibration voltage to align the beam on the coincidence camera, which may have been taken hours or days before. The thermal drift of the system necessitates that the reference alignment beam be taken immediately before the final steering voltage is calculated from the GR.

### E. Simulated Driver Beam

The simulated driver beam has been reconstructed from a Gaussian beam to provide a more stable flat-topped beam to overfill the target at the chamber center (Fig. 6). A target now occludes the driver beam very sharply, which improves the verification algorithm's precision from  $7\text{-}$  to  $2\text{-}\mu\text{m}$  stdev (for a stationary target occluding the beam). This error is not dependent on the path length of the beam but rather only on the driver beam's spatial profile and algorithm's precision. This measurement technique is helpful for measuring success on the

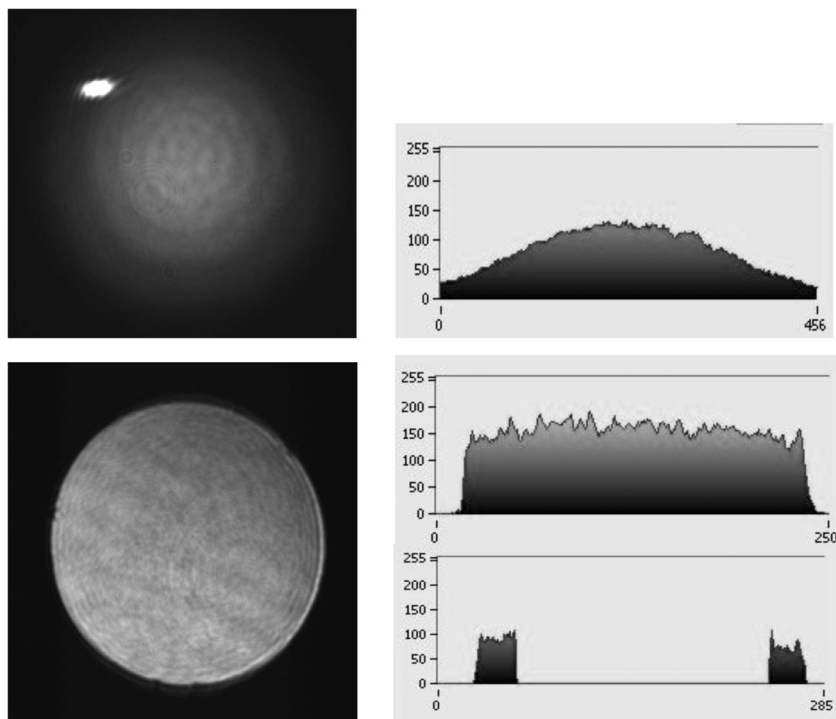


Fig. 6. (Top) Prior Gaussian driver beam with lineout. (Bottom) New flat-top driver beam with lineout of the beam and the target occluding the beam.

engagement demonstration and would potentially be used for initial testing on a full-scale startup plant.

#### IV. CURRENT ENGAGEMENT RESULTS

The current engagement result is  $34\text{-}\mu\text{m}$  stdev in vacuum with brass BBs. This represents substantial progress from the early results of  $150\ \mu\text{m}$ [4] and has been the recompense of much effort to identify and reduce the error sources one by one (Fig. 2). We want not only to reduce the error sources for the demo but also identify and understand the root causes that stand in the way of achieving our goal. Further effort will focus on understanding the effect of thermal fluctuations on the experiment and the drifting of the calibration. The engagement of lightweight targets is the next highest priority.

The question that arises concerning the promising engagement precision achieved on the tabletop demonstration is the applicability and scalability to that of a full-scale IFE system. As noted, most of our remaining errors identified in Table I are from sources that are expected to scale well to the increased distances required for an IFE power plant. Engagement must still be demonstrated at prototypic full-scale chamber distances (17 m rather than 1.5 m). Scaling the injection velocity from 5 to 50–100 m/s will require an injector with a clear sight down the trajectory, faster target positioning measurements, and faster steering mirror positioning. Faster cameras and real-time processing are feasible with current technology, at a higher cost than the demo. However, positioning full-scale steering mirrors in the available time will be more difficult and must be demonstrated. The effect of possibly turbulent high-speed chamber gas on target trajectory must also be anticipated and better understood. The path forward looks promising and attainable but is not without its intricacies.

#### REFERENCES

- [1] J. D. Sethian, M. Friedman, R. H. Lehmborg, M. Myers, S. P. Obenschain, J. Giuliani, P. Kepple, A. J. Schmitt, D. Colombant, J. Gardner, F. Hegeler, M. Wolford, S. B. Swanekamp, D. Weidenheimer, D. Welch, D. Rose, S. Payne, C. Bibeau, A. Baraymian, R. Beach, K. Schaffers, B. Freitas, K. Skulina, W. Meier, J. Latkowski, L. J. Perkins, D. Goodin, R. Petzoldt, E. Stephens, F. Najmabadi, M. Tillack, R. Raffray, Z. Dragojlovic, D. Haynes, R. Peterson, G. Kulcinski, J. Hoffer, D. Geller, D. Schroen, J. Streit, C. Olson, T. Tanaka, T. Renk, G. Rochau, L. Snead, N. Ghoneim, and G. Lucas, "Fusion energy with lasers, direct drive targets, and dry wall chambers," *Nucl. Fusion*, vol. 43, no. 12, pp. 1693–1709, Dec. 2003.
- [2] L. C. Carlson, M. Tillack, T. Lorentz, N. B. Alexander, G. Flint, D. Goodin, and R. Petzoldt, "Target tracking and engagement for inertial fusion energy—A tabletop demonstration," *Fusion Sci. Technol.*, vol. 52, no. 3, pp. 478–482, Oct. 2007.
- [3] L. C. Carlson, M. S. Tillack, J. Stromsoe, N. B. Alexander, D. T. Goodin, and R. W. Petzoldt, "Improving the accuracy of a target engagement demonstration," in *Fusion Sci. Technol.*, Jul. 2009, vol. 56, no. 1, pp. 409–416.
- [4] L. C. Carlson, M. S. Tillack, T. Lorentz, N. B. Alexander, G. W. Flint, D. T. Goodin, and R. W. Petzoldt, "Glint system integration into an IFE target tracking and engagement demonstration," *J. Phys.: Conf. Ser.*, vol. 112, no. 3, p. 032 039, 2008.



**Lane C. Carlson** received the M.S. degree in mechanical engineering from the University of California, San Diego (UC San Diego), La Jolla, in 2006.

He is currently with the Center for Energy Research, UC San Diego. He was involved in the energy research field for six years. His main research areas include demonstrating inertial fusion energy target tracking and engagement, grazing-incidence mirrors, and dry-wall chamber testing.



**Mark S. Tillack** received the Ph.D. degree in nuclear engineering from the Massachusetts Institute of Technology, Cambridge, in 1983.

He is currently the Associate Director of the Center for Energy Research, University of California, San Diego, La Jolla. He was involved in the energy research field for 26 years. His research areas include laser-matter interactions and applications of high-energy pulsed lasers as well as magnetic and inertial fusion energy technology.

**Jeremy Stromsoe** received the B.S. degree in aerospace engineering from the University of California, San Diego (UC San Diego), La Jolla.

He is currently with the Center for Energy Research, UC San Diego. He has assisted in the assembly and demonstration of inertial fusion energy target tracking and engagement, as well as electrostatic target acceleration.



**Neil B. Alexander** received the Ph.D. degree in physics from Syracuse University, Syracuse, NY.

He is currently with General Atomics, San Diego, CA. He has 20 years of experience in developing cryogenic systems for experiments on inertial confinement fusion (ICF) targets and fielding of ICF targets. He has worked on cryogenic systems to field targets on the National Ignition Facility (NIF) laser, laser welding of beryllium targets, mass production fuel layering systems for inertial fusion energy (IFE) power plants, and injection and tracking

systems for IFE power plants.

**G. W. Flint**, photograph and biography not available at the time of publication.



**Daniel T. Goodin** received the M.S. degree in radiochemistry from the University of Kentucky, Lexington.

He is currently with General Atomics, San Diego, CA. He has over 25 years of experience in fission and fusion systems development, including engineering management, inertial fusion energy targets, cryogenic engineering, tritium technology, chemical and nuclear process development, nuclear materials development, and analytical chemistry.



**Ronald W. Petzoldt** received the Ph.D. degree in applied science from the University of California, Davis.

He is currently with General Atomics, San Diego, CA. He has over 20 years of experience in the area of inertial fusion energy (IFE) research. His research areas include IFE target injection, tracking, beam pointing, electrostatic target steering, and induction accelerator design.